RSC Advances

ROYAL SOCIETY OF CHEMISTRY

www.rsc.org/advances

Highly π-extended tetrathiafulvalene analogues derived from pentacene--5,7,12,14--tetraone

Eyad A. Younes and Yuming Zhao*

Department of Chemistry, Memorial University of Newfoundland
St. John's, NL, Canada A1B 3X7

A new class of π-extended tetrathiafulvalene analogue, which is capable of reversibly revealing and concealing a central pentacene segment under redox control, was synthesized by stepwise olefination reactions on pentacene-5,7,12,14-tetraone. The structural, electronic, and redox properties were investigated by NMR, UV-Vis absorption, electrochemical analyses in conjunction with density functional theory (DFT) calculations.

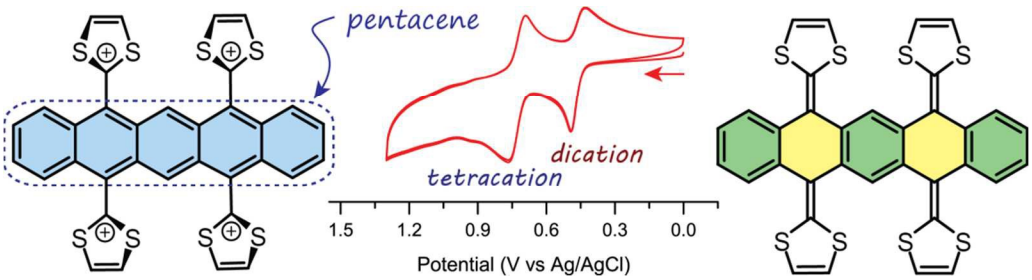

Journal Name

ARTICLE TYPE

Cite this: DOI: 10.1039/xxxxxxxxxx

Highly π–extended tetrathiafulvalene analogues derived from pentacene–5,7,12,14–tetraone†

Eyad A. Younes and Yuming Zhao*

Received Date
Accepted Date

DOI: 10.1039/xxxxxxxxxx

www.rsc.org/journalname

A new class of π–extended tetrathiafulvalene analogue, which is capable of reversibly revealing and concealing a central pentacene segment under redox control, was synthesized by stepwise olefination reactions on pentacene-5,7,12,14-tetraone. The structural, electronic, and redox properties were investigated by NMR, UV-Vis absorption, electrochemical analyses in conjunction with density functional theory (DFT) calculations.

Small-molecule semiconductors have been actively pursued in recent years, owing to their promising application in advanced molecular optoelectronic devices.[1–3] Of many organic semiconductors developed so far, fused acenes constitute a very appealing class of p–type semiconducting organic molecules; especially, pentacene-based molecules have been developed into a benchmark material for organic field effect transistors (OFETs) in light of their very high hole mobilities.[4–7] Electron–deficient acenes, on the other hand, also attract considerable attention as n–type semiconductors.[4,8] Attachment of electron–withdrawing groups, such as halogen,[9,10] cyano,[11,12] or imide groups[12–15] onto the backbone of pentacene lowers the HOMO and LUMO energies, favouring electron transport in device application. It also renders the pentacene unit to be more resistant to oxygen–caused decomposition.

Linking redox–active functional groups to various molecular/macromolecular structures is a popular design approach for generating novel functional materials with wide–ranging applications, since in this way the properties of materials can be readily modulated or tuned by straightforward redox controls.[16,17] In theory, the electronic nature of a redox–active unit can be switched between electron-donating and electron–withdrawing in different oxidation states. It is hence reasonable to assume that functionalization of pentacene with redox–active substituents would give rise to redox–switchable structural and electronic characteristics. Tetrathiafulvalene (TTF) and related π–extended analogues (i.e., exTTFs) are excellent organic electron donors, many of which can undergo facile reversible redox processes induced by electrochemical and/or chemical means.[7,18–20] A well known representative of exTTFs is the anthraquinone–derived system **1** (Scheme 1), generally referred to as TTFAQ.[7,19,21–23] In the neutral state, TTFAQ **1** adopts a non–planar saddle–like conformation.[24–27] Under moderate oxidative conditions, TTFAQ can release two π–electrons simultaneously to form a stable dication.[28–30] As depicted in Scheme 1, the two–electron oxidation transforms the central anthraquinoid unit of TTFAQ **1** into a planar anthracene structure, while the two dithiolium rings rotate to an orientation perpendicular to the central anthracene so as to minimize disfavoured charge repulsion.[7,21]

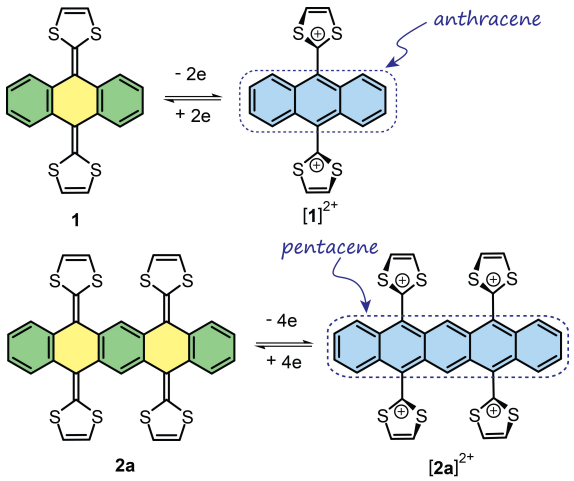

Scheme 1 Unmasking anthracene and pentacene moieties via oxidation reactions on the dithiole units in TTFAQ **1** and exTTF **2a**.

In a sense, TTFAQ can be deemed as concealing an anthracene moiety that can be fully revealed after oxidizing its two dithiole groups. The dication of TTFAQ, as a matter of fact, is an

Department of Chemistry, Memorial University, St. John's, NL A1B 3X7, Canada. Fax: 1 709 864 3702; Tel: 1 709 864 8747; E-mail: yuming@mun.ca

† Electronic Supplementary Information (ESI) available: Detailed synthetic procedures and characterization data for new compounds. See DOI: 10.1039/b000000x/

electron–deficient anthracene, given the electron–withdrawing nature of the dithiolium rings attached. Along this line, an unprecedented fused TTFAQ dimer **2a** (Scheme 1) recently caught our attention. Conceptually, compound **2a** not only represents an intriguing type of exTTFs with increased electron–donating ability compared with TTFAQ, it also exhibits an electron–deficient pentacene structure in its tetracationic state. As this type of exTTFs has not yet been known in the current literature, it is of great fundamental importance to conduct pertinent synthetic and characterization studies.

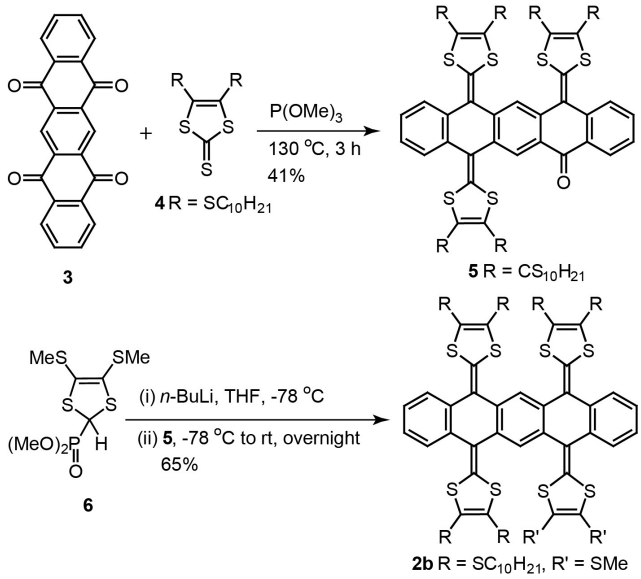

Scheme 2 Synthesis of exTTF **2b** via olefination reactions.

In this work, pentacene–5,7,12,14–tetraone (**3**)[31] was chosen as the starting material for synthesis. Initially, a fourfold $P(OMe)_3$–promoted olefination reaction[32] with thione **4** at elevated temperature (Scheme 2) was expected to directly lead to the target exTTF. However, this reaction only yielded tri–substituted compound **5** as the major product in 41% yield. Worth noting is that there were no significant amounts mono– and di–substituted products formed in this reaction. The inertness of **5** toward olefination with thione **4** can be ascribed to the strong electron–donating effects of the three dithiole groups which significantly reduce the electrophilicity of the last keto group. To accomplish the synthesis, a more reactive Horner–Wittig olefination approach was adopted, where a phosphonate ylide *in situ* generated by deprotonation of **6**[28,30] with *n*–BuLi was reacted with compound **5** to furnish the target exTTF **2b** in 65% yield.

The electronic absorption properties of exTTFs **2b** and **5** were investigated by UV–Vis spectroscopy (Fig. 1). Compound **2b** is a stable yellow coloured semisolid, and in chloroform its UV–Vis absorption spectrum exhibits four well–resolved relatively sharp peaks at 478, 401, 356, and 250 nm. In addition, two shoulder bands are discernible at 449 and 294 nm. The finely structured spectral profile is indicative of a rigid π–backbone for compound **2b**. Compound **5** is a dark–red semisolid, which shows absorption bands at 512, 418, 310 (shoulder) and 255 nm in its UV–Vis absorption spectrum. The lowest–energy absorption band of **5** is

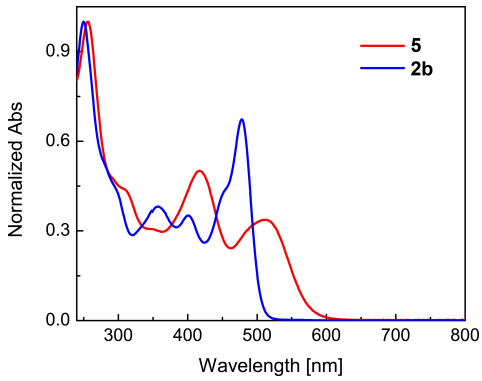

Fig. 1 Normalized UV–Vis spectra of compounds **2b** and **5** measured in $CHCl_3$ at room temperature.

considerably redshifted compared with that of exTTF **2b**, which can be attributed to the electron push–and–pull effects[33] between electron–donating dithiole groups and the electron–withdrawing ketone group in the molecular structure of **5**. This result indicates that **5** has a more narrowed HOMO–LUMO gap than **2b** does.

The redox activity of compounds **2b** and **5** were probed by cyclic voltammetric (CV) and differential pulse voltammetric (DPV) analyses (see Fig. 2). The CV profile of exTTF **2b** clearly shows two reversible redox wave pairs which are consistent with the two oxidation peaks observed at +0.46 and +0.72 V in its DPV. The results indicate that exTTF **2b** undergoes two distinctive steps of oxidation, with each step involving the transfer of two electrons given the nearly equal intensities of the two current peaks. Also worth noting is that the first oxidation potential of exTTF **2b** is significantly lower than that of a typical TTFAQ[7,28–30] by *ca*. 0.1 V, indicating that **2b** is a better electron donor than TTFAQ **1**. The DPV data of compound **5** shows three major oxidation peaks at +0.59, +0.96, and +1.21 V respectively. Together with the observation of three quasi–reversible redox wave pairs in the CV profile of **5**, the electrochemical oxidation of **5** can be attributed to three sequential single–electron transfer steps. Interestingly, there is a weak current peak observed at +0.77 V in the DPV of **5**. The origin of this peak is not quite clear at this moment and awaits further investigations to understand.

Apart from electrochemical analysis, the oxidation properties of compounds **2b** ad **5** were also studied by oxidative UV–Vis titration experiments in which a mixture of $PhI(OAc)_2/CF_3SO_3H$ (1:4 molar ratio) was utilized as the oxidant.[34] The titration results of exTTF **2b** as shown in Fig. 3 manifest two stages of spectral changes upon chemical oxidation. In the first stage (Fig. 3A), four isobestic points can be clearly seen and the lowest–energy absorption band of **2b** at 478 nm decreases substantially. A long–wavelength absorption tail ranging from 500 to 800 nm emerges and grows steadily, and this absorption feature can be ascribed to the formation of dithiolium cations during the oxidation of **2b**.[27,28,30] The second stage of spectral changes (Fig. 3B) exhibits three isobestic points, while the overall variations of spectral profiles do not appear to be as dramatic as those in the first stage. Of note is that the long–wavelength absorption tail shows a significant degree of redshift. The two–stage spectral changes observed

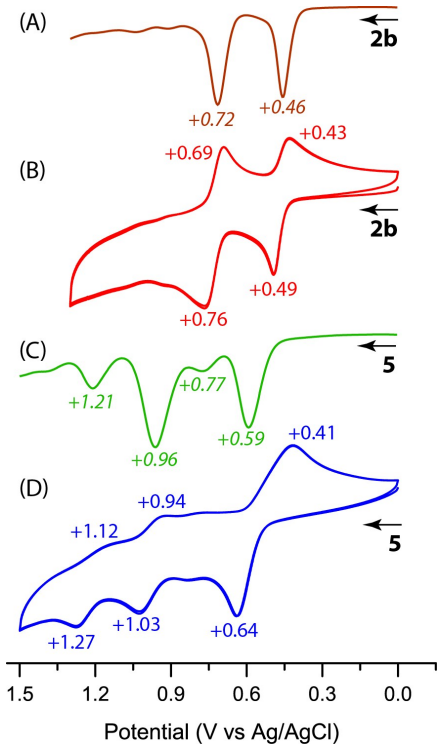

Fig. 2 Electrochemical analysis of compounds **2a** and **5** measured in CH_2Cl_2. (A) DPV of **2b**, (B) CV of **2b**, (C) DPV of **5**, and (D) CV of **5**. The arrows indicate the scan direction. Supporting electrolyte: Bu_4NBF_4 (0.1 M), working electrode: glassy carbon, counter electrode: Pt wire, reference electrode: Ag/AgCl (3 M NaCl). CV: scan rate = 100 mV s^{-1}; DPV: step = 4 mV, pulse amplitude = 50 mV, pulse width = 50 ms, pulse period = 200 ms.

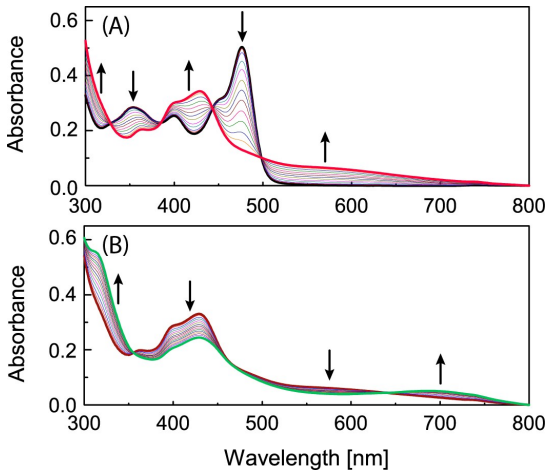

Fig. 3 UV–Vis spectra monitoring the titration of compound **2** with $PhI(OAc)_2/CF_3SO_3H$ in THF at different stages. Addition of $PhI(OAc)_2$: (A) 0 to 6.5 molecular equivalents, and (B) 7 to 14 molecular equivalents. The arrows indicate the trend of increasing oxidation.

in the oxidative UV–Vis titration of **2b** coincide with the two steps of electron transfer disclosed by electrochemical analysis. It is therefore reasonable to correlate the two stages in Fig. 3 with the formation of the dication and tetracation of **2b** in a sequential manner.

The oxidative UV–Vis titration results of compound **5** can be divided into three stages of spectral changes as depicted in Fig. 4. In the first stage, the UV–Vis absorption profile of **5** changes considerably with four isobestic points clearly seen (Fig. 4A). Unlike the case of **2b**, the characteristic long–wavelength tail of dithiolium cation is rather weak in the oxidative titration of **5**. This phenomenon is likely associated with the electron–withdrawing keto group present in the π–framework of compound **5**. In the second and third stages, the spectral profiles change only to a small extent in comparison with the first stage. In view of the stepwise single–electron transfers observed in electrochemical experiments, the three stages shown in Fig. 4 are assigned to the formation of the radical cation, dication and trication of **5** respectively.

To further understand the structural properties of exTTF **2b** in neural and oxidized states, its unsubstituted parent structure **2a** was subjected to theoretical modeling studies by the density functional theory (DTF) approach. In the neutral state, two stable conformers (denoted as *cis* and *trans*, see Fig. 5A and B) were obtained from the DFT calculations. In each of the structures, the TTFAQ segements take a saddle–like shape similar to those reported in the literature.[24–27] The two conformers differ in the positions of the dithiole rings relative to the central polyaromatic unit. Energetically, the *trans* conformer is more stable than *cis* by 0.56 kcal/mol in the gas phase. DFT calculations also indicate that the two conformers of **2a** possess very similar frontier molecular orbital properties (see ESI for details); however, the *cis* conformer has a slightly smaller HOMO–LUMO gap (4.45 eV) than *trans* (4.40 eV), as a result of its relatively higher HOMO energy. The optimized geometry of the singlet tetracation of **2a** exhibits a dramatically changed conformation in comparison with the neutral state. As expected, the central π–unit turns into a planar, fully conjugated pentacene structure, to which the four dithiolium rings are in a perpendicular orientation (Fig. 5C). The HOMO–LUMO gap of $[\mathbf{2a}]^{4+}$ is significantly reduced to 1.99 eV (in the gas phase), which accounts for the rise of a long–wavelength absorption tail in the oxidative UV–Vis titration of **2b**.

The interchange of the conformers of **2b** does not undergo a very large energy barrier, as manifested by the variable temperature (VT) NMR study. In Fig. 6, the two SCH_3 groups of **2b** clearly give a set of two singlets (2.42 and 2.43 ppm) at room temperature (298 K), suggesting that the conformers of **2b** are in rapid equilibria at kinetic rates much faster than the time scale of NMR. As the temperature decreases from 298 K to 218 K, the two SCH_3 singlets gradually merge into one broad peak. In the meantime, the range of the CH_2 proton peaks become significantly widened. This phenomenon may be related to enhanced intermolecular aggregation at lowered temperature. When the temperature is further lowered to 198 K, the broad SCH_3 peak splits into several different peaks, signifying considerably slowed down interconversion between different conformers at this temperature.

In summary, stepwise olefination reactions on pentacen–5,7,12,14–tetraone have successfully led to a new class of highly π–extended TTF analogues **2b** and **5**. The redox chemistry of these compounds features multi–stage electron transfers accompanied by dramatic conformational changes. Of great fundamen-

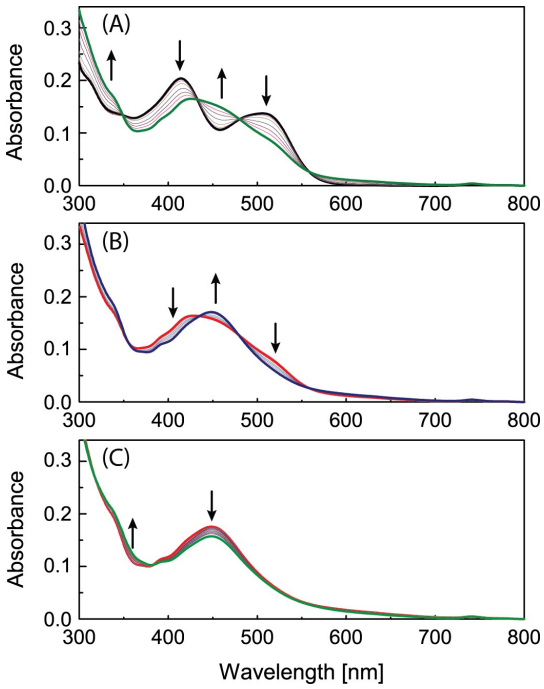

Fig. 4 UV–Vis spectra monitoring the titration of compound **5** with $PhI(OAc)_2/CF_3SO_3H$ in THF at different stages. Addition of $PhI(OAc)_2$: (A) 0 to 10 molecular equivalents, (B) 11 to 18 molecular equivalents, and (C) 19 to 36 molecular equivalents. The arrows indicate the trend of increasing oxidation.

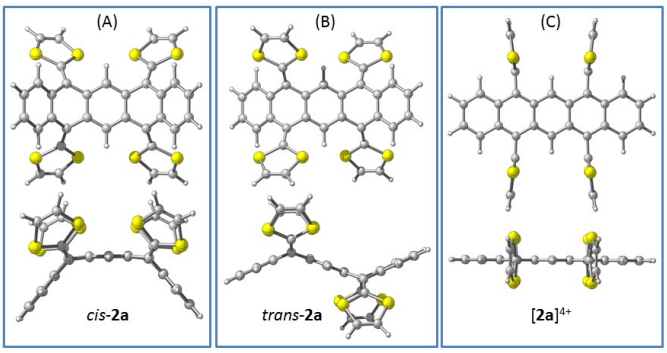

Fig. 5 Front (top) and side (bottom) views of the optimized molecular geometries of exTTF **2a** and its singlet tetracation calculated at the B3LYP/6–31G(d) level of theory.[35]

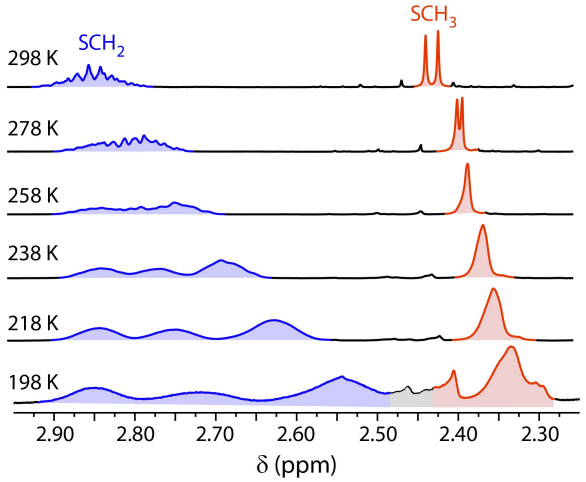

Fig. 6 Partial variable temperature (VT) ^{1}H NMR spectra (CD_2Cl_2, 500 MHz) of exTTF **2b** showing the regions of SCH_2 and SCH_3 protons.

tal interest is that the central moiety of exTTF **2b** can be transformed into a full pentacene structure after exhaustive oxidation. It is anticipated that this type of exTTFs can be developed into useful redox–switchable building blocks for advanced molecular materials and devices.

This work is financially supported by the Natural Sciences and Engineering Research Council of Canada (NSERC). Mr. Mohammadreza Khadem of Memorial University is acknowledged for assistance in VT-NMR studies.

References

1 Y. Lin, Y. Li and X. Zhan, *Chem. Soc. Rev.*, 2012, **41**, 4245–4272.
2 A. Mishra and P. Bäuerle, *Angew. Chem. Int. Ed.*, 2012, **51**, 2020–2067.
3 A. R. Murphy, and J. M. J. Fréchet, *Chem. Rev.*, 2007, **107**, 1066–1096.
4 Q. Ye and C. Chi, *Chem. Mater.*, 2014, **26**, 4046–4056.
5 J. E. Anthony, *Angew. Chem. Int. Ed.*, 2008, **47**, 452–483.
6 J. E. Anthony, *Chem. Rev.*, 2006, **106**, 5028–5048.
7 M. Bendikov, F. Wudl and D. F. Perepichka, *Chem. Rev.*, 2004, **104**, 4891–4945.
8 H. Qu and C. Chi, *Curr. Org. Chem.*, 2010, **14**, 2070–2108.
9 Y. Shu, Y.-F. Lim, Z. Li, B. Purushothaman, R. Hallani, J. E. Kim, S. R. Parkin, G. G. Malliaras and J. E. Anthony, *Chem. Sci.*, 2011, **2**, 363–368.
10 H. Qu and C. Chi, *Org. Lett.*, 2010, **12**, 3360–3363.
11 S. Katsuta, D. Miyagi, H. Yamada, T. Okujima, S. Mori, K.-i. Nakayama and H. Uno, *Org. lett.*, 2011, **13**, 1454–1457.
12 Y.-C. Lin, C.-H. Lin, C.-Y. Chen, S.-S. Sun and B. Pal, *Org. Biomol. Chem.*, 2011, **9**, 4507–4517.
13 H. Qu, W. Cui, J. Li, J. Shao and C. Chi, *Org. lett.*, 2011, **13**, 924–927.
14 Q. Ye, J. Chang, K.-W. Huang and C. Chi, *Org. lett.*, 2011, **13**, 5960–5963.
15 J. Yin, K. Zhang, C. Jiao, J. Li, C. Chi and J. Wu, *Tetrahedron Lett.*, 2010, **51**, 6313–6315.
16 G. Inzelt, *Conducting Polymers: A New Era in Electrochemistry*, Sprin, Berlin, 2nd edn, 2012.
17 *Functional Organic Materials: Syntheses, Strategies and Applications*, ed. T. J. J. Müller and U. H. F. Bunz, Wiley-VCH, Weinheim, Germany, 2006.
18 D. Canevet, M. Salle, G. Zhang, D. Zhang and D. Zhu, *Chem. Commun.*, 2009, 2245–2269.
19 J. L. Segura and N. Martín, *Angew. Chem. Int. Ed.*, 2001, **40**, 1372—1409.
20 *TTF Chemistry: Fundamentals and Applications of Tetrathiafulvalene*, ed. J.-i. Yamada and T. Sugimoto, Springer, Berlin, 2004.
21 F. G. Brunetti, J. L. López, C. Atienza and N. Martín, *J. Mater. Chem.*, 2012, **22**, 4188–4205.
22 E. M. Pérez and N. Martín, *Chem. Soc. Rev.*, 2008, **37**, 1512–1519.
23 M. R. Bryce and A. J. Moore, *Synth. met.*, 1988, **25**, 203–205.
24 R. García, M. A. Herranz, M. R. Torres, P.-A. Bouit, J. L. Delgado, J. Calbo, P. M. Viruela, E. Ortí and N. Martín, *J. Org. Chem.*, 2012, **77**, 10707–10717.
25 M. Shao, P. Dongare, L. N. Dawe, D. W. Thompson and Y. Zhao, *Org. lett.*, 2010, **12**, 3050–3053.
26 C. A. Christensen, A. S. Batsanov and M. R. Bryce, *J. Am. Chem. Soc.*, 2006, **128**, 10484–10490.
27 C. A. Christensen, M. R. Bryce, A. S. Batsanov and J. Becher, *Org. Biomol. Chem.*, 2003, **1**, 511–522.
28 M. Shao, G. Chen and Y. Zhao, *Synlett*, 2008, **2008**, 371–376.
29 N. E. Gruhn, N. A. Macías-Ruvalcaba and D. H. Evans, *Langmuir*, 2006, **22**, 10683–10688.
30 G. Chen and Y. Zhao, *Tetrahedron Lett.*, 2006, **47**, 5069–5073.
31 N. Vets, H. Diliën, S. Toppet and W. Dehaen, *Synlett*, 2006, 1359–1362.
32 C. A. Christensen, A. S. Batsanov and M. R. Bryce, *J. Org. Chem.*, 2007, **27**, 1301–1308.
33 H. Meier, *Angew. Chem. Int. Ed.*, 2005, **44**, 2482–2506.
34 M. Shao and Y. Zhao, *Tetrahedron Lett.*, 2010, **51**, 2892–2895.
35 A. D. Becke, *J. Chem. Phys.*, 1993, **98**, 5648–5652.